Biomechanics, Vol. 37, No. 5, (2004), pp. 679-687.

[11] Steinman DA: Image-based Computational Fluid Dynamics Modeling in Realistic Arterial Geometries. *Annals of Biomedical Engineering*, Vol. 30, No. 4 (2002), pp. 483-497.

[12] Liu Y, Lai Y, Nagaraj A, Kane B, Hamilton A, Greene R, McPherson DD, Chandran KB: Pulsatile Flow Simulation in Arterial Vascular Segments with Intravascular Ultrasound Images. *Medical Engineering and Physics*, Vol. 23, No. 8, (2001), pp. 583-595.

[13] Di Martino ES, Guadagni G, Fumero A, Ballerini G, Spirito R, Biglioli P, Redaelli A: Fluid-Structure Interaction within Realistic Three-Dimensional Models of the Aneurysmatic Aorta as a Guidance to Assess the Risk of Rupture of the Aneurysm. *Medical Engineering and Physics*, Vol. 23, No. 9, (2001), pp. 647-655.

[14] Funamoto K, Hayase T, Shirai A, Saijo Y, Tambe T: Fundamental Study of Ultrasonic-Measurement-Integrated Simulation of Real Blood Flow in the Aorta. *Annals of Biomedical Engineering*, Vol. 33, No. 4, (2005), pp. 415-428.

[15] Hayase T, Hayashi S: State Estimator of Flow as an Integrated Computational Method with the Feedback of Online Experimental Measurement. *Journal of Fluids Engineering-Transactions of the ASME*, Vol. 119, No. 4, (1997), pp. 814-822.

[16] Funamoto K, Hayase T, Saijo Y, Tambe T: Detection and Correction of Aliasing in Ultrasonic Measurement of Blood Flows with Ultrasonic-Measurement-Integrated Simulation. *Technology and Health Care*, Vol. 13, (2005), pp. 331-345.

[17] Funamoto K, Hayase T, Saijo Y, Tambe T: Effect of Ultrasound Probe Placement in Ultrasonic-Measurement-Integrated Simulation of Blood Flows. *Proceedings of the ICBME*, (2005), CD-ROM.

[18] Funamoto K, Hayase T, Saijo Y, Tambe T: Numerical Study on Variation of Feedback Methods in Ultrasonic-Measurement-Integrated Simulation of Blood Flow in the Aneurysmal Aorta. *JSME International Journal Series C*, Vol. 49, (2006), 144-155.

[19] Biomedical Engineering Handbook, Second Edition, Ed. Bronzino, J.D., 1 (2000), CRC Press.

[20] Chihara K: Ultrasound (in Japanese), (2001), Corona Pub. Corp.

[21] Boote EJ, Zagzebski JA: Performance Tests of Doppler Ultrasound Equipment with a Tissue and Blood-mimicking Phantom. *Ultrasound in Medicine and Biology*, Vol. 8, (1988), pp. 73-85.

[22] Fleming AD, McDicken WN, Sutherland GR, Houkins PR: Assessment of Colour Doppler Tissue Imaging Using Test-phantoms. *Ultrasound in Medicine and Biology*, Vol. 20, (1994), pp. 937-951.

[23] Rickey DW, Rankin R, Fenster A: A Velocity Evaluation Phantom for Colour and Pulsed Doppler Instruments. *Ultrasound in Medicine and Biology*, Vol. 18, (1992), pp. 479-494.

[24] Tysoe C, Evans DH: Bias in Mean Frequency Estimation of Doppler Signals Due to Wall Clutter Filters. *Ultrasound in Medicine and Biology*, Vol. 21, (1995), pp. 671-677.

[25] Willemetz JC, Nowicki A, Meister JJ: Bias and Variance in the Estimate of the Doppler Frequency Induced by a Wall Motion Filter. *Ultrasonic Imaging*, Vol. 11, (1989), pp. 215-225.

[26] Ohta M, Handa A, Iwata H, Rufenecht DA, Tsutsumi S: Poly-vinyl Alcohol Hydrogel Vascular Models for in vitro Aneurysm Simulations: The Key to Low Friction Surfaces. *Technology and Health Care*, Vol. 12, (2004), pp. 225-233.

[27] Seemantini KN, Hillary A, Greg M, Derek B, Aaron F: A Pulsating Coronary Vessel Phantom for Two- and Three-Dimensional Intravascular Ultrasound Studies. *Ultrasound in Medicine and Biology*, Vol. 29, (2003), pp. 621-628.

[28] Surry KJM, Austin HJB, Fenster A, Peters TM: Poly(vinyl alcohol) Cryogel Phantoms for Use in Ultrasound and MR Imaging. *Physics in Medicine and Biology*, Vol.49, (2004), pp. 5529-5546.

Journal of Fluid Science and Technology

Vol. 3, No. 4, 2008

Parameter Study of Hemodynamics Simulation at Internal Carotid Stenosis*

Toshio NAKAYAMA**, Hitoshi HAYASE***, Koji TOKUNAGA*** and Makoto OHTA****

**Institute of Fluid Science, Tohoku University
2-1-1 Katahira, Aoba-ku, Sendai, Miyagi 980-8577, Japan.
E-mail:nakayama@biofluid.ifs.tohoku.ac.jp

*** Neurological Surgery, Okayama University Graduate School of Medicine, Dentistry and Pharmaceutical Sciences
2-5-1 Shikata-cho, Okayama, Okayama 700-8558, Japan

**** Institute of Fluid Science, Tohoku University
2-1-1 Katahira, Aoba-ku, Sendai, Miyagi 980-8577, Japan

Abstract

Background and purpose: Stenting is one of the treatment options for carotid artery stenosis. To show the effectiveness of the treatment, computational fluid dynamics (CFD) has been performed for the last several decades. The inlet/outlet boundary conditions are important in CFD, and several researchers have used various inlet/outlet boundary conditions. In this paper, we compared the blood flow with various inlet/outlet boundary conditions and the measurement data obtained by an ultrasound device.

Methods: Blood flow speed was measured in the internal carotid artery (ICA), the external carotid artery (ECA), and the common carotid artery (CCA) using an ultrasound device. A carotid artery was reconstructed by computed tomography (CT). Mesh in the integrated data was generated to perform flow dynamics using a commercial code. CFD for blood flow was performed using the reconstructed carotid artery. Five cases of inlet and outlet boundary conditions (I/O B.C.) were used for the CFD. The simulation results were compared with the ultrasound data on the blood flow speed in the vicinity of the center of the ICA and the ECA.

Results: Various blood flow speeds were obtained from the five cases. The case of adjustment of pressures in ICA and ECA is the nearest flow speed to the ultrasound data.

Conclusion: The flow speed depends on the I/O B.C.. The I/O B.C. may be necessary for the measurement data obtained by ultrasound device or magnetic resonance imaging (MRI).

Key words: Stent, Hemodynamic, Carotid Artery, Stenosis, FVM, CFD

1. Introduction

The Cholesterols and the thrombosis pile up easily in the internal carotid artery (ICA) [(1)]. The ICA is one of the areas of predilection for stenosis [(1)]. Such stenosis may cause the decrease in cerebral blood flow and the infarct cerebral [(1)]. Poepping et al. [(2)] measured the blood flow in the carotid artery using an ultrasound device and described an in vitro system developed to obtain time-varying 3-D Doppler ultrasonic data in carotid artery bifurcation phantoms. Tada et al. [(3)] presented a three-dimensional steady numerical simulation of flow using a model of the bifurcation of the common carotid artery (CCA) into the ICA and

*Received 24 Jan., 2008 (No. 08-0044)
[DOI: 10.1299/jfst.3.544]

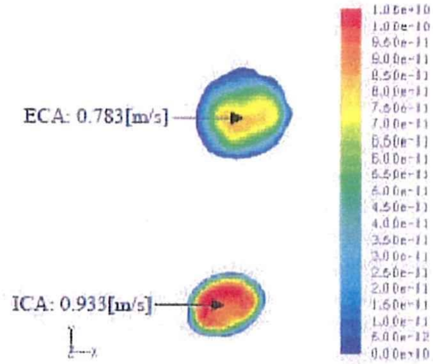

Fig.3 Velocity Contour

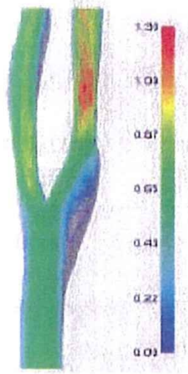

Fig.4 Streamline

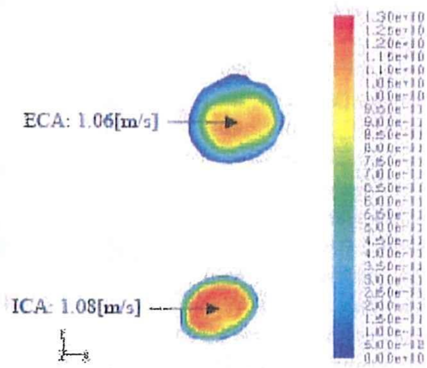

Fig.5 Velocity Contour

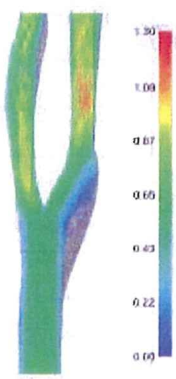

Fig.6 Streamline

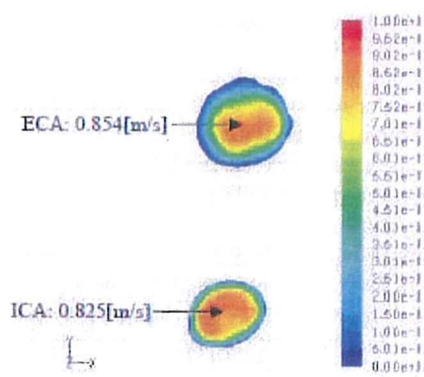

Fig.7 Velocity Contour

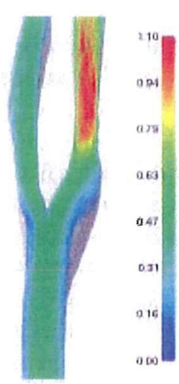

Fig.8 Streamline

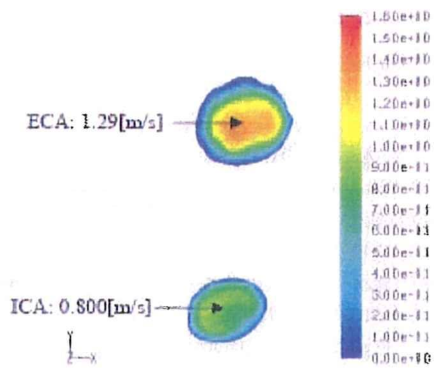

Fig.9 Velocity Contour

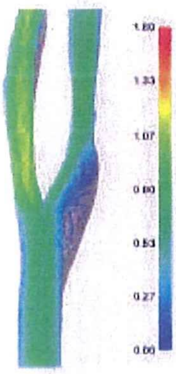

Fig.10 Streamline

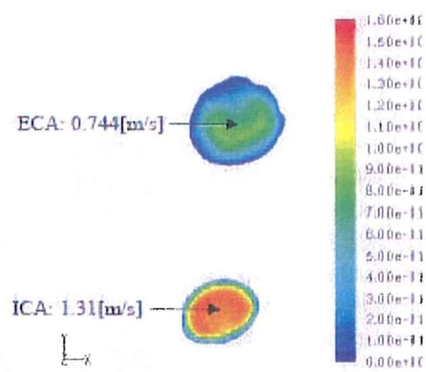

Fig.11 Velocity Contour

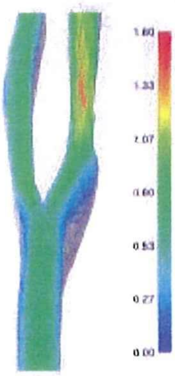

Fig.12 Streamline

Table 3 shows the blood flow speed of the ICA and the ECA and the flow speed proportions of all each cases. Table 4 shows the difference between the simulation results and the measurements data.

Table 3 Flow speed proportions

	Case 1	Case 2	Case 3	Case 4	Case 5
Velocity (ICA) [m/s]	0.933	1.08	0.825	0.800	1.31
Velocity (ECA) [m/s]	0.783	1.06	0.854	1.29	0.744
Flow speed proportion	1.19	1.03	0.955	0.618	1.76

Table 4 The difference between simulation results and measurements data

	Case 1	Case 2	Case 3	Case 4	Case 5
ICA [%]	17.00	3.67	26.65	28.83	16.28
ECA [%]	28.44	3.48	17.02	26.85	31.98

The difference between the value of simulation results and those of the ultrasound measurement of ultrasound is under 4 %. The difference of the maximum velocity in the

ECA can be decreased from 20% to 4% by adjusting the pressure at the outlet.

5. Discussion

5.1 Accuracy of calculation

In this simulation, the shapes of the simulated objects were complex. The blood vessel with the bifurcation was represented by realistic shapes at millimeter scale. Therefore, a tetrahedron mesh with a high space filling rate was selected. For a low Reynolds number such as that for the blood flow in a carotid artery, the calculation accuracy of a tetrahedron mesh was lower than that of a hexahedron mesh, and improvement of calculation accuracy will be necessary in the future.

Simulation was performed for all cases. The number of mesh elements of these cases was about 1.3 million. Although the arrangement of the tetrahedron mesh in these samples was not the same, the influence on simulation results by the difference of mesh number and arrangement of the tetrahedron mesh is thought to be small.

5.2 Influence on calculation results by the difference of I/O B.C.

In this study, we changed the I/O B.C. and investigated simulation results by difference of I/O B.C..

The outlet boundary conditions were at the set pressure outlet, the blood flow speed in the ICA was faster than that in the ECA. The flow speed balance of the ICA and ECA was equal to that of the ultrasound measurement results. The outlet boundary conditions were set the pressure and velocity outlet, the velocity of the pressure condition side was faster than the velocity condition side. The flow on the velocity condition side was not easy than the other side. The blood flow speed in the ICA and that in the ECA were greatly different from ultrasound measurements. The outlet boundary conditions were set at the velocity outlet, the flow speed balance of the ICA and the ECA was reversed. This was different from the ultrasound measurements. The ICA and ECA blood flow speed amount was slower than ultrasound measurement. From the view point of the blood flow speed and the flow speed balance of ICA and ECA, the best I/O B.C. may be Case 2 where the velocity inlet and optimal pressure outlet were set.

From the figure showing streamlines, the streamline in the carotid sinus is seen to be different due to the I/O B.C.. Rotational flow as secondary flow was occurred in the carotid sinus. We found that the size of rotational flow differed depending on the boundary conditions. Excluding Case 3, though the boundary condition of the inlet was the same, the size of the rotational flow was different. Even a main blood flow pattern of carotid artery, there was a difference in the blood flow pattern. We think that the careful boundary setting was necessary on the complex blood vessel shape.

The velocity boundary condition was calculated from the blood flow speed at the center of the blood vessel. The blood flow speed distribution in the blood vessel cross section was not obtained. The blood flow speed distribution may be necessary for the setting of velocity boundary conditions. If the blood flow speed distribution will be obtained using magnetic resonance angiography (MRA) device, we will be able to advance this research.

6. Conclusion

We simulated the blood flow in the carotid artery using several I/O B.C.. Simulation results were compared with ultrasound data and simulation results were different in all cases.

The setting of I/O B.C. made a great difference of the ultrasound measurement. The I/O B.C. may be necessary for the measurement data such as ultrasound device or MRI.

References

(1) Noda S, Himeno R, Sasahara W, Behavior of the debris in the artery stenosis, *Proceedings of the 19th Symposium on Computatuional Fluid Dynamics*, CD-ROM, 2005.

(2) Poepping TL, Nikolov HN, Rankin RN, Lee M, Holdsworth DW, An in vitro system for Doppler ultrasound flow studies in the stenosed carotid artery bifurcation., *Ultrasound Med Biol.*, Vol28, No.4, pp 495-506, 2002.

(3) Tada S, Tarbell JM, Computational Study of Flow in a Carotid Bifurcation: Geometry and Flow Ratio Correlations with WSS(Fluids Engineering), *Transactions of the Japan Society of Mechanical Engineers. B*, Vol.73, No.728, pp. 930-935, 2007. [Japanese]

(4) Naito T, Hayase T, Shirai A, Yamaguchi R, Numerical Simulation of Flow in Right Angle Branch : Mechanism of Periodical Flow Oscillation in Side Branch, *JSME annual meeting*, Vol.2000, No.1(20000731) pp. 257-258. [Japanese]

(5) Stuhne GR, Steinmanl DA, Finite-Element Modeling of the Hemodynamics of Stented Aneurysms, *Journal of Biomechanical Engineering*, Vol.126, pp381-390, 2004.

(6) Ohta M, Wetzel SG, Dantan P, Bachelet C, Lovblad KO, Yilmaz H, Flaud P, Rüfenacht DA, Rheological Changes After Stenting of a Cerebral Aneurysm: A Finite Element Modeling Approach, *CardioVascular and Interventional Radiology*, Vol. 28, pp. 768-772, 2005.

(7) Qiao A, Liu Y, Chang Y, Matsuzawa T. Computational Study of Stented Aortic Arch Aneurysms, *Proceedings of the 2005 IEEE Engineering in Medicine and Biology 27th Annual Conference*, pp.2287-2290, 2005.

(8) Birchall D, Zaman A, Hacker J, Davies G, Mendelow D, Analysis of haemodynamic disturbance in the atherosclerotic carotid artery using computational fluid dynamics, *European Radiology*, Vol.16, pp.1074-1083, 2006.

(9) Tori R, Oshima M, Kobayashi T, Takagi K, Tezduyar TE, Influence of wall elasticity in patient-specific hemodynamic simulations, *Computers & Fluids*, Vol.36, Issue 1, pp. 160-168, 2007.